

Operation Characteristics of Small-DC-Current, Applied-Field MPD Thruster

*Presented at Joint Conference of 30th International Symposium on Space Technology and Science
34th International Electric Propulsion Conference and 6th Nano-satellite Symposium,
Hyogo-Kobe, Japan
July 4 – 10, 2015*

Daisuke Ichihara¹, Tomoki Uno², Hisashi Kataoka², Akira Iwakawa³ and Akihiro Sasoh⁴
Nagoya University, Nagoya, Aichi, 464-8603, Japan

Abstract: Cylindrical and rectangular shaped applied field magnetoplasmadynamic thruster (Af-MPD) were developed and investigated operation characteristics under small discharge current. For cylindrical shape the thrust was huge affected by anode radius. As common tendency, measured thrust showed similar trend to Swirl acceleration model or theoretical Lorentz force by putting cathode at near the anode exit surface.

Nomenclature

B	=	magnetic flux density at coil center for cylindrical shape, acceleration channel center for rectangular shape
B_{exit}	=	magnetic flux density at anode exit surface of cylindrical shape
F	=	thrust
F_{theory}	=	theoretical Lorentz force of rectangular shape
F_{Swirl}	=	theoretical force by Swirl acceleration of cylindrical shape
H	=	inter electrode distance of rectangular shape
J_d	=	discharge current
J_k	=	keeper current
\dot{m}	=	propellant mass flow rate
R_a	=	anode radius of cylindrical shape
R_c	=	cathode radius of cylindrical shape
V_d	=	discharge voltage
V_k	=	keeper voltage
$z_{\text{cathode tip}}$	=	cathode tip position

I. Introduction

ELECTRODE erosion and lower thruster performance of the magneto-plasma-dynamic (MPD) thruster are the most important technical problems to realize high power electric propulsion in the near future.¹⁻³⁾

MPD thruster is able to be classified into two types by operating principal. Self-field MPD (Sf-MPD) thruster uses induced magnetic field by discharge current J_d and thrust is proportional to J_d^2 . Therefore, several tens kA discharge current is required and input power needs more than one mega-watt. This power range is outside the reach of power level which can make in space. On the other hand, Applied-field MPD (Af-MPD) thruster uses external magnetic field B by solenoid coil or permanent magnets. The thrust is proportional to $J_d B$ or $J_d B^2$ ⁴⁾. Therefore, the thrust can be increased with magnetic field increasing even if the discharge current is small. From these reasons, we

¹ Student, Department of Aerospace Engineering, Ichihara@fuji.nuae.nagoya-u.ac.jp.

² Student, Department of Aerospace Engineering

³ Assistant Professor, Department of Aerospace Engineering, iwakawa@nuae.nagoya-u.ac.jp.

⁴ Professor, Department of Aerospace Engineering, sasoh@nuae.nagoya-u.ac.jp.

propose small current operation of Af-MPD thruster. Although the small current can decrease Joule heating and suppress cathode erosion, the conventional rod cathode cannot maintain the discharge since the lack of the electron emission capability. Hence, thermionic emission type hollow cathode which keeper electrode is redesigned is used instead of conventional rod cathode⁵⁾. Hollow cathode enables to make adequate amount of thermionic electrons for easy ignition and long stable operation with small current.

In this study, the operation characteristics of a cylindrical and a rectangular type Af-MPD thruster under small current operation are measured respectively. Thrust and discharge voltage are measured varying with propellant mass flow rate, discharge current, applied magnetic field strength, cathode position, and anode diameter of cylindrical type Af-MPD thruster.

II. Experimental setup

A. MPD thruster head

In this experiment, two size of anode radius type (small and large) cylindrical Af-MPD thruster were developed. The schematic images of the small and large type cylindrical Af-MPD thruster are illustrated in Fig. 1 and Fig. 2 respectively. In both type thruster, the discharge channel is consist of cylinder shape, water cooled anode and hollow cathode. Anode inner radius of the small type cylindrical Af-MPD thruster is variable for 15 and 20 mm and that of large type cylindrical Af-MPD thruster is 40 mm fixed. As mentioned above, hollow cathode was installed instead of conventional rod cathode. The hollow cathode is consisted of commercially available cathode tip (Kaufman & Robinson Inc.) and newly developed keeper electrode with 2 mm diameter orifice. The hollow cathode position $z_{\text{cathode tip}}$ is variable along the central line. The propellant (Argon) was fed to the discharge channel through hollow cathode. In both size of cylindrical Af-MPD thruster, external magnetic field was applied to the discharge channel by water cooled solenoidal coil. The magnetic flux density was 266 mT at the center of the coil.

In the next place, The schematic of the MPD thruster is illustrated in Fig. 3. The rectangular discharge channel width and length are 20 mm and 60 mm, respectively. The inter-electrode distance, H , is varied from 5 to 15 mm. The upper wall is water cooled anode made of copper. On the lower wall, a hollow cathode which almost same configuration as cylindrical one but orifice diameter is 3 mm, was also mounted. The cathode The propellant (Argon) was fed to the discharge channel through hollow cathode. An external magnetic field was applied to the discharge channel by two neodymium magnets connected with an iron yoke. The magnetic flux density was 200 mT at the center of the discharge channel ($z_{\text{cathode tip}} = 19\text{mm}$). In order to change the magnetic flux density, relative position between magnets and discharge channel was changed.

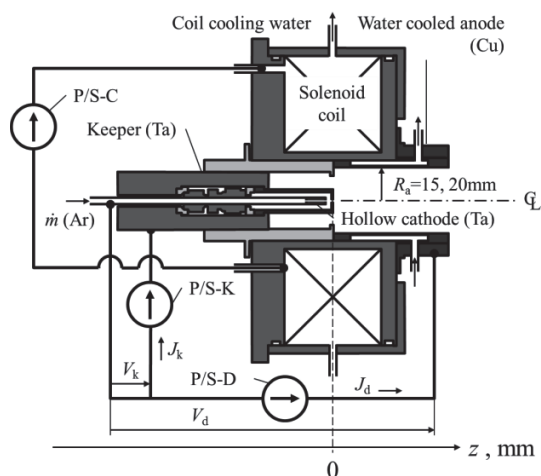


Figure 1 Schematic image of small size cylindrical MPD thruster

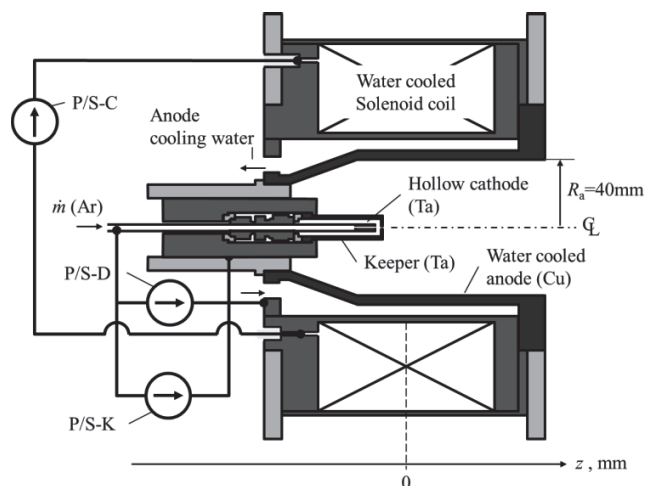


Figure 2 Schematic image of large size cylindrical MPD thruster

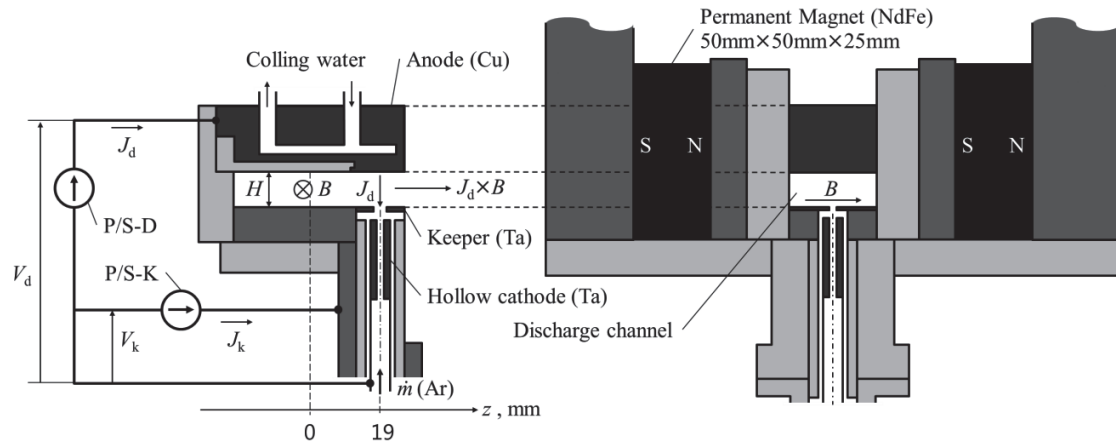


Figure 3 Schematic image of rectangular MPD thruster

B. Vacuum system and measurement system

The experiments in this study were conducted in a vacuum chamber whose diameter and length are 2 m and 4m respectively (Figure 3). The vacuum chamber is evacuated using a turbo molecular pump (3200L/s) backed by a rotary pump (33.3L/s). The ambient pressure in the vacuum chamber was measured by an ionization vacuum gauge and a pirani gauge. The ambient pressure without propellant flow was 10^{-3} Pa; at the mass flow rate of 1.25 mg/s, ambient pressure was 7.0×10^{-2} Pa.

Thrust was measured using a pendulum type thrust stand. It consists of a stand arm, a vacuum bellows and two radial bearings. A differential transformer is used to detect the pendulum oscillation amplitude. The thrust was estimated by this differential transformer signal considering tare force. Thrust, discharge voltage and keeper voltage were measured varying propellant mass flow rate, discharge current, magnetic flux density, anode radius for cylindrical shape Af-MPD thruster, inter-electrode distance for rectangular shape Af-MPD thruster. These data were logged using DL-750 (Yokogawa Electric Corporation).

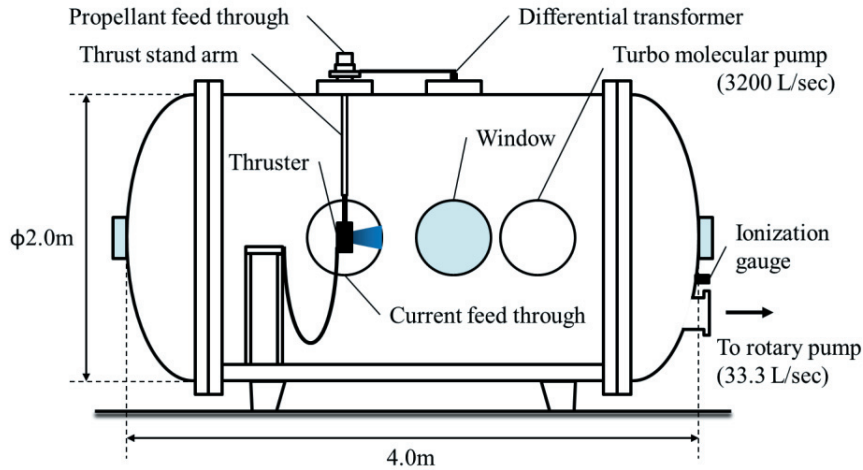


Figure 4 Vacuum system

III. Experimental results

A. Operation condition

The operation condition of both cylindrical and rectangular shape Af-MPD thrusters are tabulated on Table 1. Propellant was six nines Argon.

Table 1 Operation condition

Control parameter	Symbol	Small size cylindrical	Large size cylindrical	Rectangular
Total mass flow rate [mg/s]	\dot{m}	0.41-2.1	0.41-2.1	0.41-2.1
Discharge current [A]	J_d	5-15	5-15	5-15
Applied magnetic field [mT]	B	114-265	132-265	200, 230
Keeper current [A]	J_k	2	2	2
Anode radius [mm]	R_a	15, 20	40	
Inter electrode distance [mm]	H			5-15
Cathode tip position [mm]	$z_{\text{cathode tip}}$	0-70	0-80	19

B. Influence of \dot{m}

Figure 5 shows F and V_d of cylindrical shape Af-MPD thruster as a function of \dot{m} . As shown in this figure, F was almost independent on \dot{m} and as decreasing \dot{m} , discharge voltage increased. This tendency is opposite of Arc jet thruster which is type of electro thermal acceleration and indicates that the electromagnetic acceleration is dominant in this operation region. Figure 6 shows F of rectangular shape Af-MPD thruster as a function of \dot{m} . The tendency is similar as cylindrical one but thrust increased as decreasing \dot{m} . This tendency leads to the suggestion that V_d increment must be caused by the increment of the back electromagnetic force.

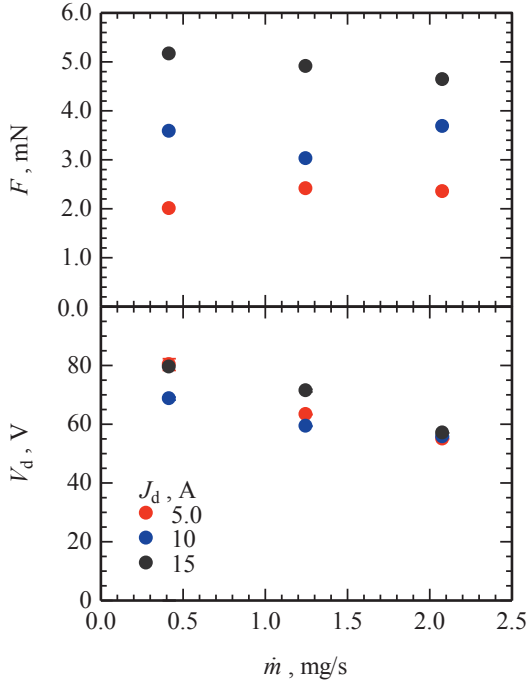


Figure 5 F and V_d of cylindrical type Af-MPD thruster as a function of \dot{m} . $J_d=5-15$ A, $B=265$ mT, $R_a=15$ mm, $z_{\text{cathode tip}}=0$ mm.

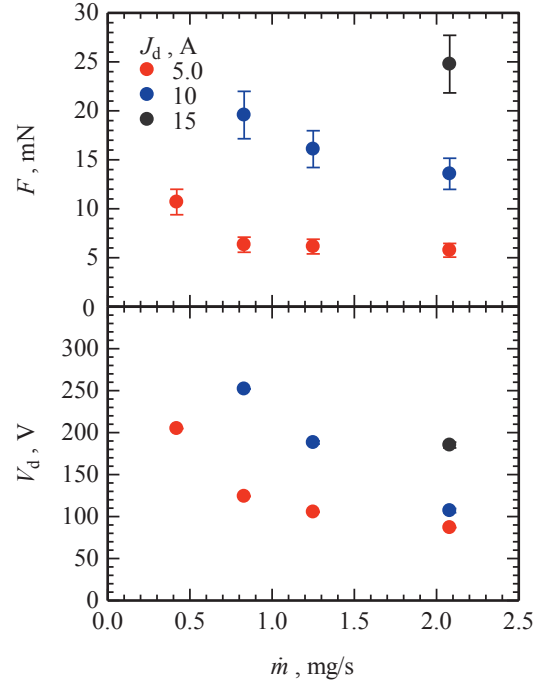


Figure 6 F and V_d of rectangular type Af-MPD thruster as a function of \dot{m} . $J_d=5-15$ A, $B=200$ mT, $H=10$ mm, $z_{\text{cathode tip}}=19$ mm.

C. Influence of J_d and B

Figure 7 and **Figure 8** shows F and V_d of cylindrical shape and rectangular shape Af-MPD thruster as a function of J_d and also, **Figure 9**, **Figure 10** shows F and V_d as a function of B respectively. Both thrusters showed same tendency that as J_d and B increasing, F and V_d increased linearly and especially in the rectangular shape Af-MPD thruster, thrust was proportional to J_d . From these results, it leads to the suggestion that increasing $J_d B$ led to increase thrust.

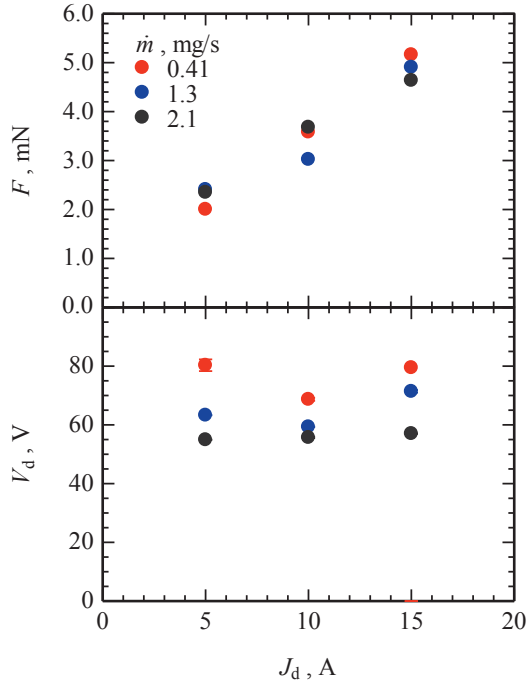


Figure 7 F and V_d of cylindrical type Af-MPD thruster as a function of J_d . $\dot{m}=0.41\text{-}2.1\text{mg/s}$, $B=265$ mT, $R_a=15$ mm, $z_{\text{cathode tip}}=0\text{mm}$.

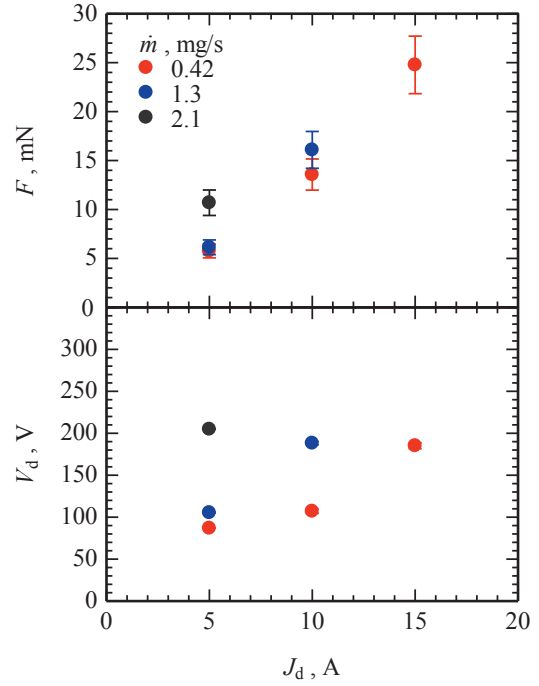


Figure 8 F and V_d of rectangular type Af-MPD thruster as a function of J_d . $\dot{m}=0.41\text{-}2.1\text{mg/s}$, $B=200$ mT, $H=10$ mm, $z_{\text{cathode tip}}=19\text{mm}$.

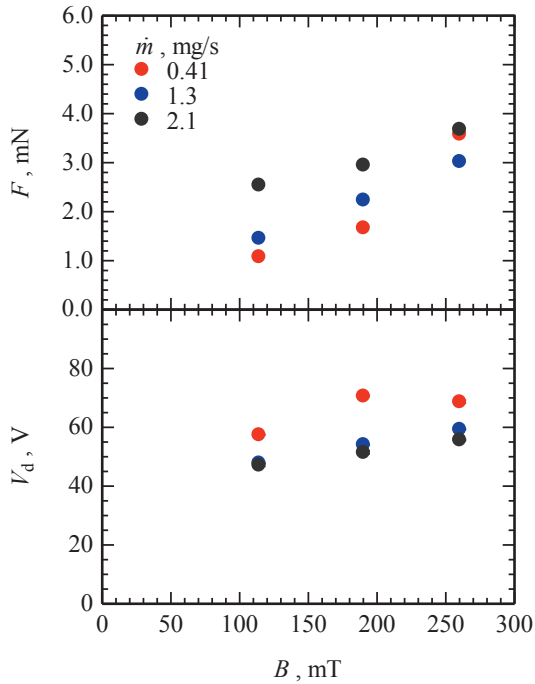


Figure 9 F and V_d of cylindrical type Af-MPD thruster as a function of B . $\dot{m}=0.41\text{-}2.1\text{mg/s}$, $J_d=5\text{-}15$ A, $R_a=15$ mm, $z_{\text{cathode tip}}=0\text{mm}$.

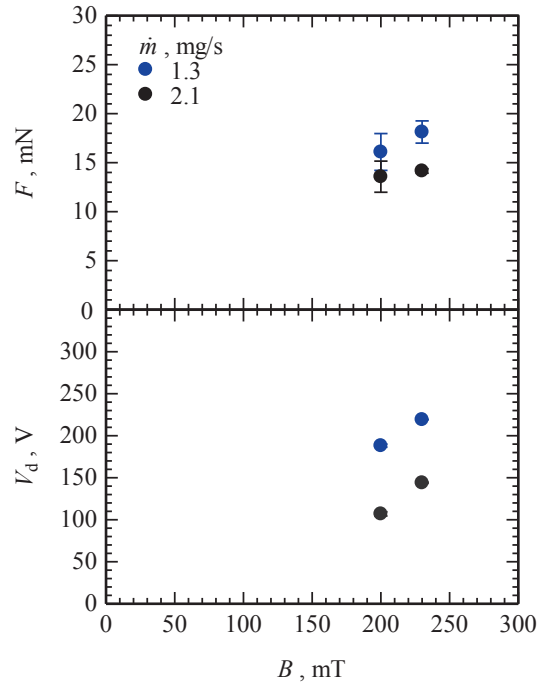


Figure 10 F and V_d of rectangular type Af-MPD thruster as a function of B . $\dot{m}=0.41\text{-}2.1\text{mg/s}$, $J_d=5\text{-}15$ A, $H=10$ mm, $z_{\text{cathode tip}}=19\text{mm}$.

D. Influence of $z_{\text{cathode tip}}$.

The discharge current distribution is well affected by relative position between anode and cathode. In order to increase thrust, F and V_d was measured as cathode position $z_{\text{cathode tip}}$ of cylindrical shape Af-MPD thruster changing and Fig. 11 shows the results. As shown in this figure, V_d was not changed so much. However, F increased as increasing $z_{\text{cathode tip}}$. Especially in $\dot{m}=2.1\text{mg/s}$, F increased 1.5 times as varying $z_{\text{cathode tip}}$ from 0 to 70 mm. This is because of decrement of thrust loss to discharge channel surface.

E. Influence of R_a

Figure 12 shows F and V_d of cylindrical Af-MPD thruster as a function of \dot{m} . With constant \dot{m} , F increased drastically as R_a increasing especially in $\dot{m}=0.41\text{mg/s}$, F increased more than 3 times from $R_a = 15$ mm to 40 mm. Increasing R_a leads to increase volume to surface ratio of acceleration area and as a result, the thrust losses to the discharge channel wall decreased.

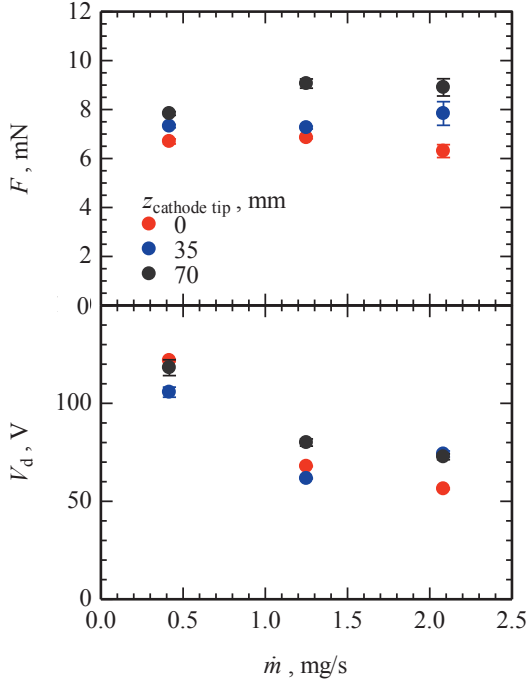


Figure 11 F and V_d of cylindrical type Af-MPD thruster as a function of $z_{\text{cathode tip}}$. $\dot{m}=0.41\text{mg/s}$, $J_d=10$ A, $B=265$ mT, $R_a=15$ mm.

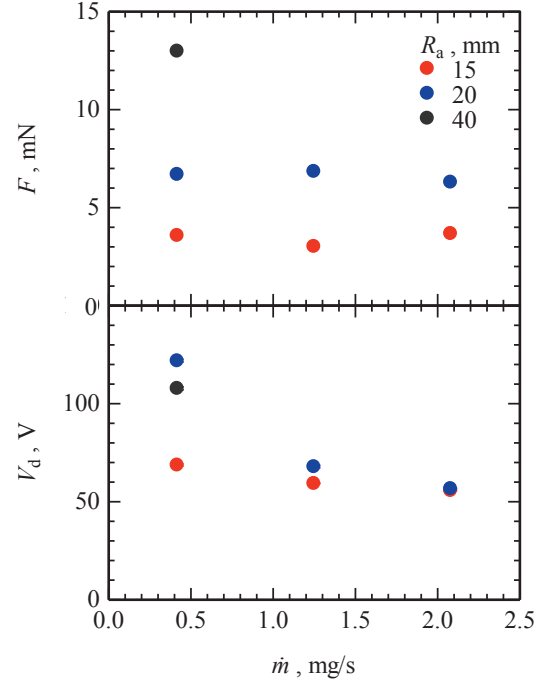


Figure 12 F and V_d of cylindrical type Af-MPD thruster as a function of R_a . $\dot{m}=0.41\text{mg/s}$, $J_d=10$ A, $B=265$ mT, $z_{\text{cathode tip}}=0\text{mm}$.

F. Compare to theoretical value

In above sections, the influence of each operation condition to thrust and discharge voltage is discussed. In this section, the relationship between experimental value and theoretical one is focused. Under operation condition summarized in Table 1, self-fild acceleration or thermal acceleration is ignorable. In this case, Hall acceleration or Swirl acceleration can be dominant to make thrust. Insofar as cylindrical shape Af-MPD thruster, exhaust plume diverted along the lines of magnetic field and also, some part of plume was rotating. From these observation, Swirl acceleration is dominant. The theoretical thrust formula of Swirl acceleration is represented as

$$F_{\text{swirl}} = \frac{1}{\sqrt{2}} J_d B_{\text{exit}} R_a \left[1 - \frac{3}{2} \left(\frac{R_c}{R_a} \right)^2 \right] \quad (1)$$

where B_{exit} is magnetic flux density at anode exit and R_c is cathode radius, respectively. Here, R_c is equal to orifice radius (1.0mm). From Eq. (1), F_{swirl} is proportional to discharge current, magnetic flux density and anode radius. Figure. 13 shows F of cylindrical shape Af-MPD thruster as a function of $J_d B_{\text{exit}} R_a$ and F_{swirl} is also plotted. When cathode was set at anode exit surface ($z_{\text{cathode tip}} = 70$ mm for small type and $z_{\text{cathode tip}} = 80$ mm for large type cylindrical shape Af-MPD thruster), thrust was bigger than $z_{\text{cathode tip}} = 0$ mm. Also, thrust tendency to

$J_d B_{\text{exit}} R_a$ is similar as F_{Swirl} . However, as $J_d B_{\text{exit}} R_a$ increasing, F showed another trend against theoretical formula and the thrust value was smaller than F_{Swirl} . This is because thrust loss to the discharge channel wall or constant angular momentum which assumed in Swirl acceleration theory was not achieved under this operation conditions.

On the one hand, the theoretical Lorentz force F_{theory} of rectangular shape Af-MPD thruster is represented as

$$F_{\text{theory}} = J_d B H \quad (2)$$

Figure. 14 shows F of rectangular shape Af-MPD thruster as a function of $J_d B H$ and F_{theory} and previous study results⁶⁾ are also plotted. As shown in this figure, thrust increased by setting hollow cathode at near the anode exit surface ($z_{\text{cathode tip}} = 19$ mm) and reached almost 90% of F_{theory} . This is because thrust losses to keeper electrode resolved by changing cathode position.

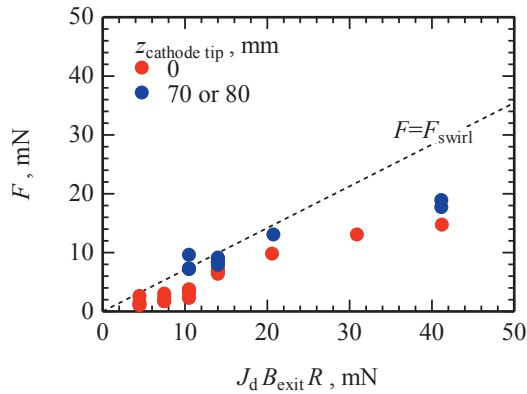


Figure 13 F of cylindrical type Af-MPD thruster as a function of $J_d B_{\text{exit}} R_a$. $\dot{m}=0.41\text{-}2.1\text{mg/s}$, $J_d=5\text{-}15$ A, $B_{\text{exit}}=52\text{-}103$ mT, $R_a=15\text{-}40$ mm.

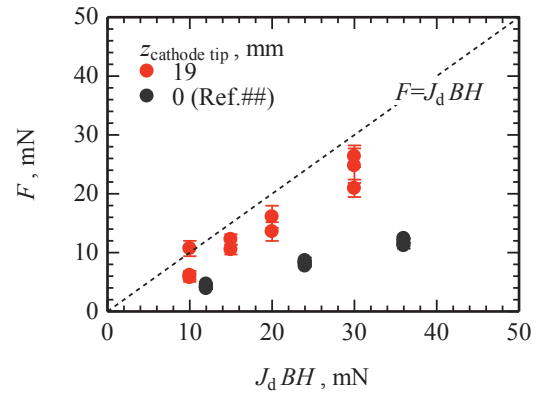


Figure 14 F of rectangular type Af-MPD thruster as a function of $J_d B H$. $\dot{m}=0.41\text{-}2.1\text{mg/s}$, $J_d=5\text{-}15$ A, $B=200$ mT, $H=10$ mm. Reference values are also plotted.

IV. Conclusion

Cylindrical and rectangular shape Af-MPD thruster were developed and investigated operation characteristics of each thruster. As common tendency, thrust increased linearly as increased discharge current and magnetic flux density. In cylindrical Af-MPD thruster, anode radius have a huge effect on thrust and increased more than 3 times by increased anode radius from 15 mm to 40 mm. Measured thrust value were compared to theoretical one and by setting hollow cathode at near the anode exit surface, thrust tendency is similar to Swirl acceleration theory or theoretical Lorentz force.

References

- ¹ M. Auwetwe-Kurtz et al. "Optimization of Electric Thrusters for Primary Propulsion Based on the Rocket Equation," IEPC01-181.
- ² K. Toki et al. "Application of MPD Thruster System to Interplanetary Missions," AIAA Paper-85-2026.
- ³ E. Choueiri "On the Thrust of Self-Field MPD Thrusters," IEPC Paper 97-121.
- ⁴ A. Sasoh, "Thruster Performance and Acceleration Mechanisms of Steady-State, Applied-Field MPD Arcjets", Ph.D. thesis, TheUniversity of Tokyo, (1989).
- ⁵ G. Krulle et al. "Technology and Application Aspects of Applied Field Magnetoplasmadynamic Propulsion" Journal of Propulsion and Power, 14, 5 (2009) pp. 754-763.
- ⁶ S. Yokota et al, "Steady-State, Applied-Field, Rectangular MPD Thrusters", IEPC Paper 2013-246.